

Theoretical Modeling of Pulsed Plasma Thruster Performance with Teflon Ablation

Mingyoung Cho* and Hong-Gye Sung**

Department of Aerospace and mechanical engineering, Korea Aerospace University, Goyang 10540, Republic of Korea

Abstract

A performance analysis for a pulsed plasma thruster(PPT) has been conducted to predict the thrust and current change. Two models were implemented - a one-dimensional lumped circuit analysis model and the Teflon ablation model provided by Michael Keidar. The circuit model incorporating resistance and inductance models was adapted to predict the magnitude of the discharge current. Numerical simulations like current discharge rates with different voltages were reasonably well compared with experimental data. The effects of Teflon ablation on thruster characteristics were investigated.

Key words: Pulsed plasma thruster, Teflon ablation, Lorentz force

Nomenclature

- β : correction factor
- Φ_B : Magnetic flux (Vs)
- μ_0 : Magnetic permeability of free space (N/A²)
- Γ_i : Ion erosion rate (kg/C)
- B : Magnetic field (T)
- C_{PPT} : Capacitance of the PPT (F)
- h : Separation distance between electrodes (m)
- I : Current (A)
- J : Current Density (A/m²)
- k : Boltzmann constant (J/K)
- L : Inductance (H)
- m : Atomic mass of Teflon (kg)
- \dot{m} : Mass flow rate (kg/sec)
- n : Number density (1/m³)
- P : Pressure (Pa)
- T : Temperature (K)
- V : Voltage applied across the Capacitor (V)
- R : Resistance (Ω)

Subscripts

Capacitor : Properties of Capacitor

Circuit : Properties of Circuit
 Plasma : Properties of plasma
 0 : initial value

1. Introduction

A pulsed plasma thruster (PPT), a plasma jet engine, is a form of electric spacecraft propulsion. PPTs are generally cheap to manufacture and to operate. In addition, they are mechanically scalable. The efficiency of the thruster is, however, lower than chemical propulsion systems. A typical PPT consists of several constituent components; propellant, a

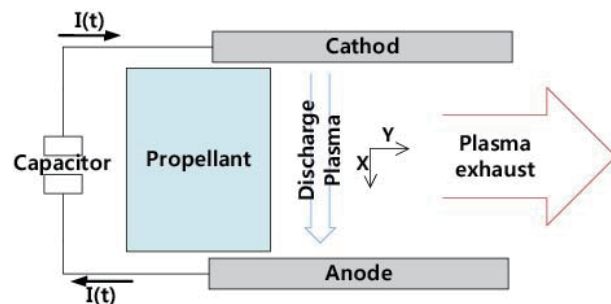


Fig. 1. Schematic of a PPT

This is an Open Access article distributed under the terms of the Creative Commons Attribution Non-Commercial License (<http://creativecommons.org/licenses/by-nc/3.0/>) which permits unrestricted non-commercial use, distribution, and reproduction in any medium, provided the original work is properly cited.

© * PhD. Candidate student
 ** Professor, Corresponding author: hgsung@kau.ac.kr

capacitor storing energy, a power unit to supply the capacitor with energy, electrodes accelerating the forming plasma, and a sparkplug to initiate the discharge as shown in Fig.1

PPT system analysis models require specific physics different from chemical propulsion systems because of a plasma flow to produce thrust. For PPT systems, an analysis must be carried out on the interaction between the propellant surface and the plasma bulk and the motion of plasma flow through nozzle.

The purpose of the present study is to develop in-house modeling capabilities to understand a pulsed plasma discharge. A one-dimensional lumped circuit analysis model with a MHD flow model method was implemented. A lumped circuit model including plasma resistance and inductance model was adapted to predict the magnitude of a discharge current. Using Newton's second law and Lorentz force, the motion of the plasma bulk was predicted. The Teflon ablation was analyzed using Micheal Keidar's model. [1] The effect of the Teflon ablation on the thruster characteristics were investigated. The PPT model also predicted the current profile for discharges between electrodes and the analysis results were validated with previous research.

2. Governing Equations

2.1 Momentum equation

To predict the acceleration of the plasma bulk as a whole out of the thruster, Newton's second law and Lorentz force were adapted.

$$\frac{d}{dt}(m_{tot}v) = \frac{dm_{tot}}{dt}v + m_{tot}\frac{dv}{dt} = \int_V J \times BdV \quad (1)$$

where v is the velocity of the plasma and dm_{tot}/dt is the mass flow rate of plasma when a discharge occurs. The plasma bulk consists of copper, carbon and fluorine ions separated from electrodes and Teflon gas from a propellant surface. The rate of mass loss of copper can be determined as a function of the discharge current(I) and the ion erosion rate(Γ_i).

$$\frac{dm_{tot}}{dt} = \Gamma_i I + \dot{m}_{Teflon} \quad (2)$$

When evaluating Lorentz force, the magnetic field contribution from the self-induced magnetic field in the x-y plane will cancel itself out, so only the external magnetic field in the y-axis needs to be considered. In the present study, the external magnetic field in the x-axis was zero as the fringe effects are neglected. The current density in the x-y plane is also zero. The Lorentz force integrated over the cylindrical coordinates can be therefore calculated using

[2]. Φ is a half of an electrode's thickness and I_z is current through an electrode.

$$\int_V J \times BdV = \frac{\mu_0 I_z}{2\pi} \log \frac{2h}{\phi+h} \quad (3)$$

The Eqs. 1 through 3 can be summarized and expressed as Eq. 4.

$$\begin{aligned} (\Gamma_i I + \dot{m}_{Teflon}) \frac{dx}{dt} + \frac{d^2x}{dt^2} \left(\Gamma_i \int_0^t I dt + \int_0^t \dot{m}_{Teflon} dt \right) \\ = \frac{\mu_0 I_z}{2\pi} \log \frac{2h}{\phi+h} \end{aligned} \quad (4)$$

The modeling of the Teflon ablation rate and the current value generated during the discharge is required to calculate the motion of the plasma flow using Eq. 4. To predict the current value, the lumped circuit model is utilized. In order to predict the amount of Teflon ablation, the theoretical model proposed by Micheal Keidar is adapted. [1]

2.2 Lumped circuit model

A current of the PPT system flows through the current loop. It can be alternatively expressed as the difference between the potential before and after the current discharge. Also, by considering Kirchhoff's law, the electromotive force can be expressed as Eq. 5

$$\begin{aligned} V_0 - \frac{1}{C_{PPT}} \int I dt \\ = IR_{circuit} + L_{circuit} \frac{dI}{dt} + I \frac{dL_{circuit}}{dt} \end{aligned} \quad (5)$$

where V_0 is the applied voltage and C_{PPT} is the magnitude of the capacitor supplying power to the thruster. The circuit inductance and resistance, respectively, can be expressed as,

$$L_{circuit} = L_{capacitor} + L_{electrode} + L_{plasma} \quad (6)$$

$$R_{circuit} = R_{capacitor} + R_{electrode} + R_{plasma} \quad (7)$$

The inductance of the plasma(L_{plasma}) is determined by the magnetic flux moving through the plasma. However, for a closed surface, the magnetic flux is zero.

$$L_{plasma} = \frac{\phi_B}{I} = \frac{1}{I} \oint B dS = 0 \quad (8)$$

The inductance and resistance values of the capacitor were obtained experimentally. These values are changed according to which capacitor model is being applied to the system. The inductance and resistance of the electrode is changed according to the induced current generated in the electrode. Both parameters could be estimated via modeling them. To calculate the resistance of the plasma generated between the electrodes, a simplified MHD equation was used. [3]

2.3 Teflon ablation model

In a PPT, a discharge occurs between two electrodes across the propellant. A heat flux is propagated from the plasma to the Teflon surface during the discharge. The ablated vapor which is made by the heat transport is ionized near the propellant surface and is accelerated by the electromagnetic force. To formulate proper boundary condition for the overall boundary model and predict performance of the thruster, it is important to choose a model which is reasonable for describing the plasma-propellant surface interaction.

As shown in Fig.2, sub-regions near the surface can be sorted two regions by the different physical phenomena - Knudsen layer and non-equilibrium ionization region (NEIR). These sub-regions express the entire transition region between the equilibrium plasma and the wall. The area to the right side of the boundary 3 is the region which satisfies the quasi-neutrality.

Micheal Keidar proposed the theoretical model to analysis the relation between the Knudsen layer and the hydrodynamic non-equilibrium layer. [1] The model is the distribution function of the emitted particles which is transformed from a half-Maxwellian into a drifted Maxwellian at the Knudsen edge. The relations between parameters at the Knudsen layer edge can be described by the following set of following equations[4].

$$\frac{n_0}{2(\pi d_0)^{0.5}} = n_1 V_1 + f1(\alpha) \tag{9}$$

$$\frac{n_0}{4d_0} = \frac{n_1}{4d_1} (1 + 2\alpha^2 + f2(\alpha)) \tag{10}$$

$$\frac{n_0}{(\pi d_0)^{1.5}} = \frac{n_1}{\pi d_1^{1.5}} (\frac{\alpha}{4} + \alpha^3 + f3(\alpha)) \tag{11}$$

where,

$$f1(\alpha) = \beta \frac{n_1(\exp(-\alpha^2) - \alpha\pi^{0.5}\text{erfc}(\alpha))}{2(\pi d_1)^{0.5}}$$

$$f2(\alpha) = \beta \frac{(0.5 + \alpha^2)\text{erfc}(\alpha) - \alpha \exp(-\alpha^2)}{\pi^{0.5}}$$

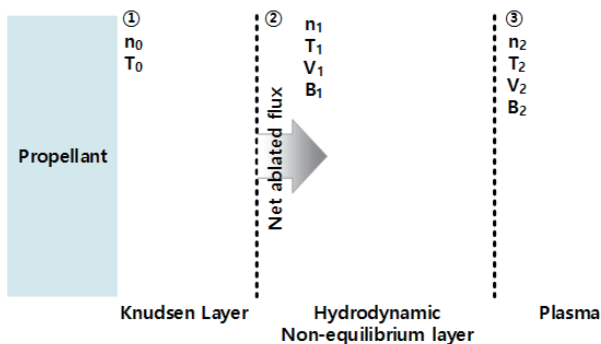


Fig. 2. Schematic zoomed in near surface layer

$$f3(\alpha) = \frac{\beta(\frac{\alpha}{4} + \alpha^3)\text{erfc}(\alpha) - (2 + \alpha^2)\exp(-\alpha^2)}{2\frac{\pi^{0.5}}{V_1}}$$

$$\alpha = \frac{V_1}{2kT_1/m}, \quad d_0 = \frac{m}{2kT_0}, \quad d_1 = \frac{m}{2kT_1}$$

$$fc(\alpha) = 1 - \text{erf}(\alpha), \quad \text{erf}(\alpha): \text{error function}$$

T_0 is the surface temperature, T_1 is the Knudsen layer temperature, and n_0 is the equilibrium density. The velocity at the edge of the Knudsen layer remains a free parameter in these equations. To find the velocity V_1 , the combination of the mass and momentum equations at boundary 2 and 3 yields the following expression for the velocity at the outer boundary of the Knudsen layer.

$$\frac{V_1^2}{2kT_1/m} = \frac{(T_2 n_2 / 2T_1) - (n_1 / 2)}{n_1 - (n_1^2 / n_2)} \tag{12}$$

$$P_0 = n_0 k T_0 = P_c \exp\left(-\frac{T_c}{T_0}\right) \tag{13}$$

where $P_c = 1.84 \times 10^{15} \text{ N/m}^2$, $T_c = 20,815 \text{ K}$

P_0, P_c and T_c are the equilibrium pressure, the characteristic pressure, and temperature respectively.

3. Analysis Algorithm

Eqs. 4 and 5, representing the plasma motion and discharge current, can be expressed using a differential equation with time. In this study, the Runge-Kutta 4th order integration method was used to predict changes in the current between electrodes and the flow of the plasma bulk. Variables to govern the equations, including the circuit resistance and inductance values, were calculated for each subroutine used the main routine in the PPT performance analysis.

If Eq. 9 through 12 are used to determine the solution for ablation rate at every time-step, the computing time would increase rapidly. To reduce the calculation time, this study

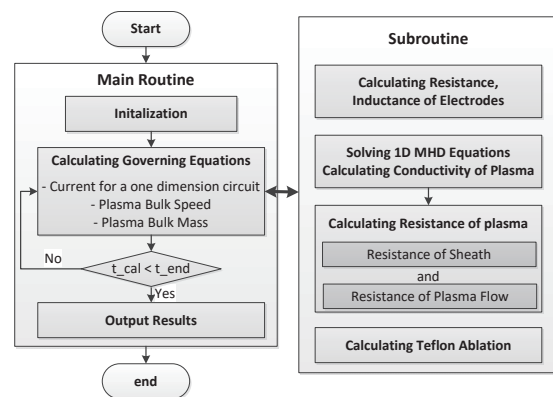


Fig. 3. Flow chart for the PPT performance analysis

organized the solutions from Eqs. 9 to 12 in tabular form. The Teflon ablation rate was determined via interpolation. This is standard procedure, and it is carried out using the temperature and density of plasma for each time step. The resistance of the plasma bulk is solved from the inverse of the conductivity integrated across the distance between the electrodes. Plasma conductivity is a function of plasma frequency and density. To gain plasma properties such as electron temperature, plasma density and flow velocity, a simplified one- dimensional MHD equation is adapted. Fig. 3 shows a flow chart for the PPT performance analysis.

4. Discussion

4.1 Validation

The analysis results are compared with experimental data[2] for discharge current variation between the electrodes as measured during PPT operation. Teflon serves

Table 1. PPT specifications

High Voltage Capacitor	
Capacitance (μF)	4.06
Charging Voltage (V)	596,952,1229,
Cap. Inductance (nH)	310
Cap. Inductance (m Ω)	33
Electrode	
Width (mm)	20
Thickness (mm)	10
Discharge Channel Length(mm)	60
Separation (mm)	30

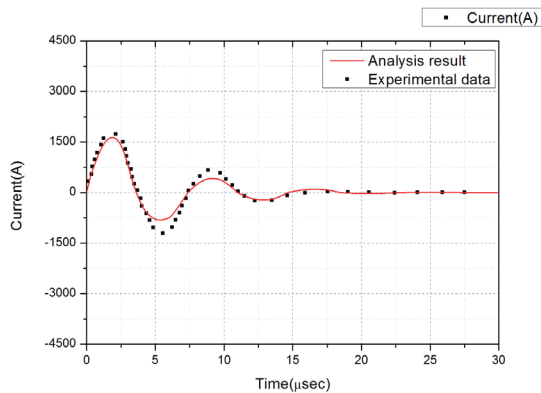


Fig. 4. Comparison result with experimental data ($V_0=596\text{V}$)

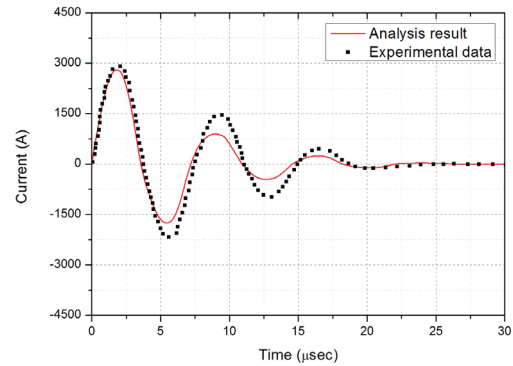


Fig. 5. Comparison result with experimental data ($V_0=952\text{V}$)

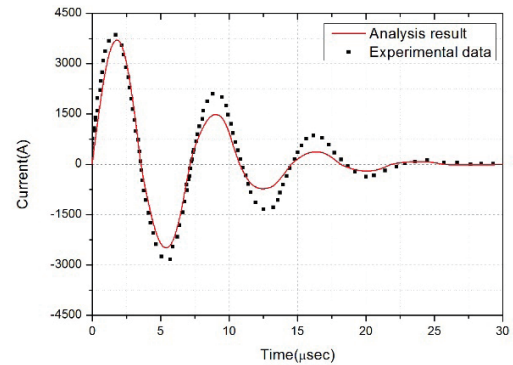


Fig. 6. Comparison result with experimental data ($V_0=1229\text{V}$)

as the PPT propellant and it is inserted between the two electrodes. Table 1 shows the PPT specifications.

Figures 4, 5 and 6 show the validity of the model in terms of predicting the current profile with Teflon ablation at 596V, 952V and 1229V at an electrode gap separation of 3cm. Current discharge rates with different voltages are compared with experimental data. Both the experimental and calculated results have the same frequency about 134kHz. The sinusoidal wave is gradually offset due to the intermittent current discharge between electrodes. The decrease in the current magnitude gained from analysis results is faster than decrease in the current of the experimental data since the ionization of the Teflon gas is not considered in this study.

4.2 Prediction of Plasma flow

Figures 7 through 9 show the prediction of the discharge current properties at 1229V. The distribution of the electron density and the temperature rapidly increases to these peak and then gradually decays. A tendency of two results are similar because the electron temperature effects on an ionization of copper molecules and ions. The maximum value of the electron temperature is 254eV. Because it is enough energy to raise Cu^{+25} charge state, the plasma density

is dense at high temperature region. This phenomenon was observed by the previous experimental study.[6]

Figure 9 shows the flow radius distribution of the plasma flow between the electrodes during the discharge. The flow radius shows a conical expansion from the cathode surface to the anode surface before reaching the maximum current. When the discharge current decreases, the minimum value

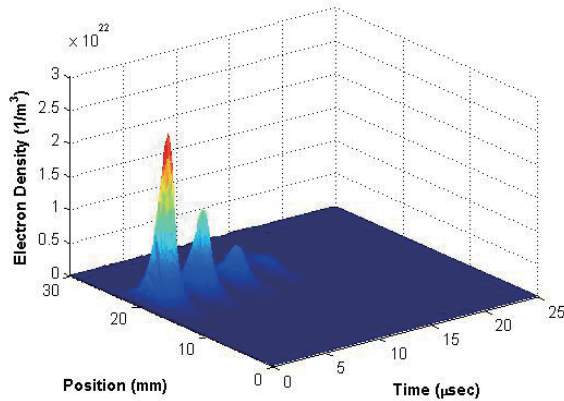


Fig. 7. Electron density

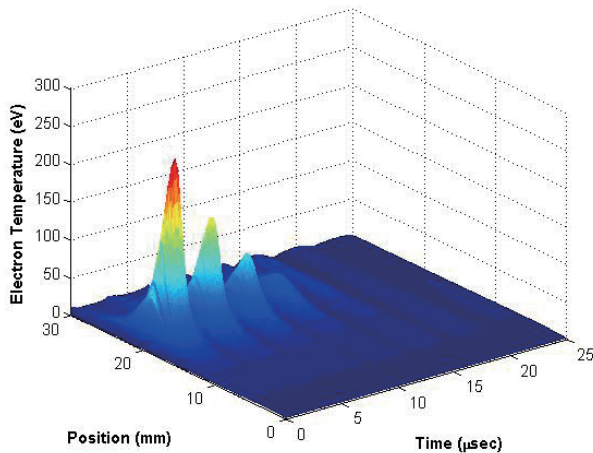


Fig. 8. Electron temperature

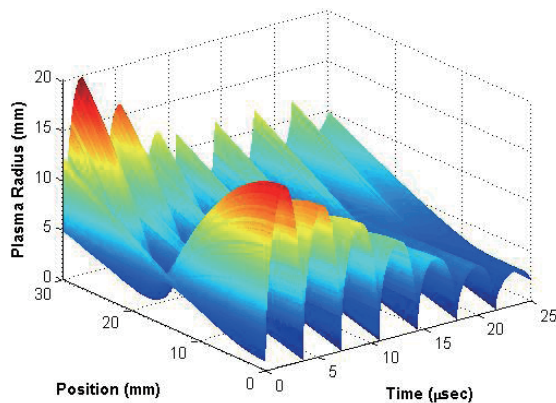


Fig. 9. Plasma Radius

of the plasma radius is located between the electrodes because of the electron density decrease and the plasma radius gradually decays because of same reason.

4.3 Comparison results with/without Teflon ablation

The predicted PPT performance with and without the Teflon ablation is compared. The plasma flow, which was caused by the current discharge and Teflon ablation, accelerates due to the Lorentz force. Because the thrust of a PPT system is function of the mass flow rate and the velocity of gas, Teflon ablation rate is an important factor for

Table 2. Thrust with/without Teflon ablation

$V_0 = 596V$	Teflon ablation	
	w/	w/o
F_{max} (μN)	1.15	0.53
	117.0% increase	
F_{mean} (μN)	0.22	0.12
	83.3% increase	
$V_0 = 952V$	Teflon ablation	
	w/	w/o
F_{max} (μN)	3.38	1.54
	119.5% increase	
F_{mean} (μN)	0.73	0.39
	87.2% increase	
$V_0 = 1229V$	Teflon ablation	
	w/	w/o
F_{max} (μN)	5.82	2.67
	118.0% increase	
F_{mean} (μN)	1.39	0.73
	90.4% increase	

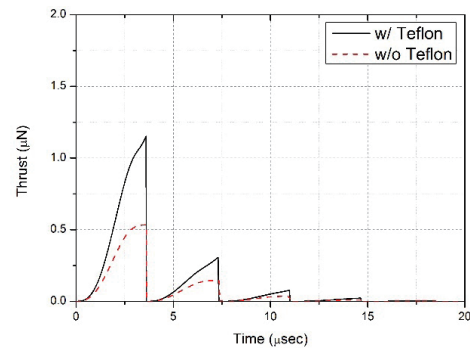


Fig. 10. Comparison results with/without Teflon ablation ($V_0=596V$)

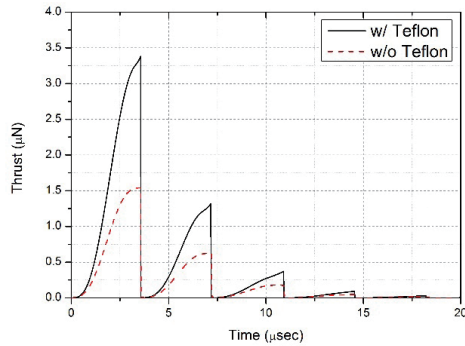


Fig. 11. Comparison results with/without Teflon ablation ($V_0=952V$)

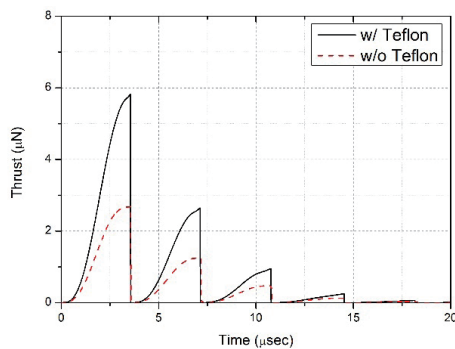


Fig. 12. Comparison results with/without Teflon ablation ($V_0=1229V$)

determining the PPT performance. Figs. 10 through 12 show the thrust from each of the analytical results.

Compared to the thrust without Teflon ablation, the thrust with Teflon ablation increases about 120%, and the average thrust increases about 83%–90%. When the charging voltage increases, the difference becomes more. The rise of plasma kinetic energy gained from the discharging process can promote the rate of Teflon ablation.

5. Conclusions

The analysis model of PPT performance is developed which is based on a 1-D lumped circuit model including the ablation rate of Teflon and the behavior of the plasma flow using MHD equation. The Micheal Keider's model is implemented for plasma properties and Teflon ablation rates. A detailed analysis of the discharge electrode based on

splitting the conductor is conducted.

The validation of the model in terms of predicting the current profile with Teflon ablation at 596V, 952V and 1229V has an electrode gap separation of 3cm. Both the experimental and calculated results have very similar current profile and the same frequency about 134kHz. The tendency of the electron temperature and the ion number density are similar because the electron temperature affects on an ionization of copper molecules and ions.

Teflon ablation augments thrust about 120% over the ignoring of Teflon ablation and the increment is positively proportional to the charging voltage. In addition, a plasma kinetic energy gained from the discharging could promote the Teflon ablation rate and the maximum thrust.

Acknowledgement

This work was supported by grant from the National Research Foundation of Korea (NRF-2015M1A3A3A02104484).

References

- [1] Keidar, M., Boyd, I. D. and Beilis, I. I., "On the Model of Teflon Ablation in an Ablation Controlled Discharge", *Journal of Physics D, Applied Physics*, Vol. 34, 2001, pp. 1675-1677.
- [2] Shaw, P. V., "Pulsed Plasma Thrusters for Small Satellites", Doctoral Thesis, University of Surrey, 2011.
- [3] Krinberg, I. A., "Plasma Flow Crisis and the Limiting Electron Temperature in a Vacuum Arc in Axial Magnetic Field", *Technical Physics Letters*, Vol. 31, No. 3, 2005, pp. 261–263.
- [4] Keidar, M., Boyd, I. D. and Beilis, I. I., "Ionization and Ablation Phenomena in an Ablative Plasma Accelerator", *Journal of Physics*, Vol. 96, No. 10, 2004, pp. 5420-5428.
- [5] Keidar, M. and Boyd, I. D., "Plasma Engineering", *Elsevier*, 2013, pp. 68-76.
- [6] Artamonov, M. F., Krasov, V. I. and Paperny, V. L., "Registration of Accelerated Multiply Charged Ions from the Cathode Jet of a Vacuum Discharge", *Journal of Experimental and Theoretical Physics*, Vol. 93, No. 6, 2001, pp. 1216-1221.